Mapping the Climats Change Impact on Land Cover and Land Surface Temperature in Hashimiya District, Using Remote Sensing Data.

1.Elaf Amer Alyasiri Ph.D, Department of Geography, College of Education and Human Sciences, University of Babylon, Hillah, Iraq.
Email: Ealyasiri@uobabylon.edu.iq | ORCID: 0000-0001-8002-4683
2. Ameen Awad Kadhim Ph.D, Department of Apply Geography, College of Education and Human Sciences, University of Karbala, Karbala, Iraq.
Email: Ameen.a@uokerbala.edu.iq | ORCID 0000-0003-0229-4287
3.Adnan Karim Kahar, Department of Geography, College of Education and Human Sciences, University of Babylon, Hillah, Iraq.
4. Diyaa Bahij Rauf, Department of Geography, College of Education and Human Sciences, University of Babylon, Hillah, Iraq.

Abstract:
This study investigates land cover change (LCC) and land surface temperature (LST) in the Hashimiya district for the years 2015 and 2025 to evaluate the impact of climate change. Landsat 8 data from these years were utilized as input data. Water, vegetation, and impervious surface indices were applied to map LCC, while land surface temperature was analyzed to assess the urban heat effect in Hashimiya. The findings were compared with NASA Power data for validation; however, the results did not align.
The study revealed a slight decrease in the Water Index (WI), which declined from 1.1% in 2015 to 1% in 2025. Conversely, the Vegetation Index (VI) experienced a minor decline, dropping from approximately 53.5% in 2015 to 53.3% in 2025. The Impervious Surface Index (IS) indicated an upward trend, with the coverage of impervious surfaces increasing from 45.4% in 2015 to 45.5% in 2025. Additionally, the study measured land surface temperature (LST), which ranged from 55°F (12.7°C) to 65°F (18.3°C) in 2015, and increased to a range between 65°F (18.3°C) and 75°F (23.8°C) in 2025. This demonstrates an increase in LST of approximately 5 degrees.

Key Words*: Land Surface Temperature (LST), NDVI, NDISI, NDWI, Climate Change.*

التمثيل الخرائطي لتأثير التغير المناخي على الغطاء الأرضي ودرجة حرارة سطح الأرض في قضاء الهاشمية باستخدام بيانات الاستشعار عن بعد

١. ا.م.د. إيلاف عامر الياسري، قسم الجغرافيا، كلية التربية للعلوم الإنسانية، جامعة بابل، الحلة، العراق.
Email: Ealyasiri@uobabylon.edu.iq | ORCID: 0000-0001-8002-4683
٢. ا.م.د. امين عواد كاظم ، قسم الجغرافيا، كلية التربية للعلوم الإنسانية، جامعة كربلاء، الحلة، العراق.
Email: Ameen.a@uokerbala.edu.iq | ORCID 0000-0003-0229-4287
٣. م.د. عدنان كريم كهار ، قسم الجغرافيا، كلية التربية للعلوم الإنسانية، جامعة بابل، الحلة، العراق.
٤. ا.م.د. ضياء بهيج رؤوف ، قسم الجغرافيا، كلية التربية للعلوم الإنسانية، جامعة بابل، الحلة، العراق.

الملخص:
تبحث هذه الدراسة في العلاقة بين تغييرات الغطاء الأرضي (LCC) ودرجة حرارة سطح الأرض (LST) في قضاء الهاشمية للمدة الزمنية ٢٠١٥ و٢٠٢٥ وذلك لتقييم تأثير تغييرات المناخ على الغطاء الارضي. تم استخدام بيانات القمر لاندست ٨ من هاتين السنتين كبيانات مدخلة. تم تطبيق مؤشرات الماء والنباتات والأسطح غير النفاذة لرسم خارطة تغير الغطاء الارضي ، بينما تم تحليل درجة ءحرارة سطح الأرض لتقييم تأثير الحرارة الحضرية في الهاشمية. تمت مقارنة النتائج مع بيانات NASA Power للتحقق من صحتها .كشفت الدراسة عن انخفاض طفيف في مؤشر الماء (WI)، الذي انخفض من ١,١% في ٢٠١٥ إلى ١% في ٢٠٢٥. أما مؤشر النباتات (VI) فقد شهد انخفاضًا طفيفًا، حيث انخفض من حوالي ٥٣,٥% في ٢٠١٥ إلى ٥٣,٣% في ٢٠٢٥. أشار مؤشر الأسطح غير النفاذة (IS) إلى زيادة طفيفة، حيث زادت تغطية الأسطح غير النفاذة من ٤٥,٤% في ٢٠١٥ إلى ٤٥,٥% في ٢٠٢٥. بالإضافة إلى ذلك، قامت الدراسة بقياس درجة حرارة سطح الأرض (LST)، التي تراوحت بين ٥٥ (12.7°C) °F و٦٥ (18.3°C) °Fفي عام ٢٠١٥، وزادت إلى نطاق بين ٦٥ °F (18.3°C)و ٧٥ (23.8°C) °Fفي عام ٢٠٢٥. وهذا يظهر زيادة في درجة حرارة سطح الأرض بحوالي ٥ درجات.

1. Introduction

Climate change refers to prolonged changes in temperature, precipitation, wind patterns, and other elements of Earth's climate system. It includes global warming and shifts in weather patterns, along with an increase in the frequency and severity of hurricanes, heat waves, floods, and droughts. These changes can impact both natural ecosystems and human societies (*What Is Climate Change? - NASA Science*, 2025). As temperatures increase, the melting of polar ice results in rising sea levels and pushes ecosystems beyond their capacity. Vulnerable species face challenges due to habitat loss and rapid environmental changes, which can affect biodiversity and ecosystem services. Additionally, climate change imposes significant challenges on agriculture, water availability, and human health, while also posing threats to economic stability and global security. The increasing frequency of extreme weather events necessitates communities globally address more frequent natural disasters through robust adaptation and resilience strategies (Nouban & Abazid, 2017). The increase in greenhouse gas emissions from activities such as burning fossil fuels has led to a noticeable, steady rise in land surface temperatures over the past century. Regions with vast landmasses warm more rapidly than areas dominated by oceans. This differential warming is not just a statistical trend—it has real-world consequences. Warmer land surfaces can exacerbate drought conditions, alter local weather patterns, and impact agriculture and natural ecosystems. In many regions, particularly arid ones, this means that the heat is not only increasing averages but also intensifying the extremes, leading to more frequent and severe heatwaves (Climate Change Impacts on Land Temperature Increase, 2025.)

Land Surface Temperature (LST) is an essential metric that indicates the warmth of the Earth's surface layer, akin to the temperature one would feel upon direct contact. Distinct from near-surface air temperature, which is measured by meteorological stations, LST is evaluated through satellite sensors that detect thermal infrared radiation emitted by various surfaces. Consequently, LST accurately represents temperature variations across different terrains, whether it be a snow-covered expanse, a sunlit concrete sidewalk, a forest canopy, or a cultivated crop field. (Land Surface Temperature, NASA Earth, 2025.) The utilization of Land Surface Temperature (LST) data encompasses various fields, including climate research, agriculture, and urban planning. Researchers examine LST patterns to investigate land–atmosphere interactions, focusing on the exchange of heat, water, and energy. This information is essential for comprehending the effects of increasing greenhouse gases on climate trends. Furthermore, practical applications involve evaluating crop water requirements during periods of heat stress or pinpointing urban areas susceptible to heat island phenomena (Land Surface Temperature, 2025).Land Surface Temperature (LST) is a critical factor for studying the impact of Climate Change (CC) on the Earth's physical and chemical factors. It contains the effects of atmosphere and ground to interact between the surface and the atmosphere. The most crucial issue facing the globe, especially in urban areas, is the increase in surface temperature caused by transforming vegetated areas into impermeable areas, as well as the conversion of wetlands and vegetated areas into agricultural land or barren wastelands. These changes affect the amount of solar radiation absorbed, surface temperature, heat transfer to the soil, and the near surface atmosphere (Mallick et al., 2008). It also impacts on energy and water balance and effect on environmental processes (Oke & Cleugh, 1987; Pal & Ziaul, 2017).

Growing populations and expanding cities impact the environment, as urbanization brings about various environmental problems and contributes to climate change. With increasing populations, the demand for housing, industries, roads, and other infrastructure changes the land cover of the region (Sun et al., 2017). Urbanization has significantly altered land cover patterns over the past 20 years (Khandelwal et al., 2018). These changes have resulted in increases in

LST in cities, where the average temperature is 2-5°C higher than in nearby villages or districts. These thermal islands affect urban hydrology and the environment. Detecting changes in LC and spatial mapping are essential tools for identifying spatial and temporal variations in an area (Ullah et al., 2019; Khandelwal et al., 2018).
Changes in land cover and their impacts on the environment are becoming significant global issues (K. Li et al., 2020a; Qin & Karnieli, 1999; Rasul et al., 2018). According to United Nations projections, by 2050, 69% of the global population could be at risk from rising Land Surface Temperature (LST) and various pollutants. In 2022, the world's population was about 8 billion. It is expected to grow by approximately 2 billion over the next thirty years, reaching around 9.7 billion by 2050. By the mid-2080s, the population is anticipated to be nearly 10.4 billion (United Nations, 2024). In recent decades, multispectral imagery, various remote sensing data, and GIS techniques have become widely available as sources for a better understanding of the various elements of the Earth's environment, mapping LC and calculating LST (Hart & Sailor, 2009; Zha et al., 2003; Al Rakib et al., n.d.; Zhang et al., 2017; Avdan & Jovanovska, 2016; Alyasiri 2024;).
The main goal of this study is to detect the impact of the environmental change on LST and LC in Hashimiyafor the selected periods (2015 and 2025) in various types of LC, including vegetation, water, and impervious surface area.

2. Related research

Researchers have been using remotely sensed data and GIS techniques to investigate the impact on LST and LC since the 1960s. The study of LST dynamics has significantly improved computational methods using remote sensing data and various sensors.
Joshi et al. (2024) investigates the correlation between the Normalized Differential Vegetation Index (NDVI) and Land Surface Temperature (LST) in Dehradun over the past two decades. The analysis uses LST, NDVI, and temperature data obtained via remote sensing from various Landsat satellite series (L5, L7, and L8) spanning 1991 to 2021. To determine the distribution of healthy vegetation, shrublands/grasslands, and water/snow cover over time, the processed NDVI data were classified accordingly. The relationship between LST and NDVI classes of healthy vegetation, shrublands/grasslands, and water/snow cover was examined both before and after the monsoon season. Pengaruh et al. (2024) focuses on Cox's Bazar district, which is characterized by its evolving land use patterns and vulnerability to the Urban Heat Island effect. Utilizing GIS and RS techniques, the research examines the dynamics of Land Use and Land Cover (LULC), Land Surface Temperature (LST), Normalized Difference Vegetation Index (NDVI), and Normalized Difference Built-Up Index (NDBI) from 1990 to 2020. The analysis reveals significant changes in LULC, with implications for environmental degradation and sustainable management.Patel et al. (2024) Urbanization-driven changes in Land Use and Land Cover (LULC) affect Land Surface Temperatures (LSTs) and outdoor thermal comfort. Although urban heat stress on thermal comfort has been extensively studied, the impact of LULC remains under-researched.Tanoori et al. (2024) examines how urban configuration affects the distribution of heat, known as the Urban Heat Island effect, in Shiraz, Iran. Various Machine Learning algorithms are used to analyze LST data across different land cover types, including built-up areas, soil, and vegetation. Additionally, the study evaluates the impact of specific configuration metrics within each land cover category. This approach helps identify which urban morphology features most significantly influence LST. The findings can guide targeted interventions and management strategies to reduce heat and enhance thermal comfort in specific areas of Shiraz.
Mansourmoghaddam et al. (2024) This study evaluates Land Surface Temperature (LST) in the city of Yazd, Iran, where field data and high-resolution thermal images are limited. LST is analyzed using surface indices derived from Landsat-8 satellite images for two contrasting seasons winter and summer of 2019 and 2020. Subsequently, LST is estimated for the year 2021.
Al Shawabkeh et al. (2024) Higher LST in cities compared to their surrounding areas presents a significant sustainability challenge for urban environments. Decision-makers and planners use

LST measurements to monitor urban conditions and address the primary challenges of urban climates. The study focused on the relationship between LST and urban land changes and the impact of these changes on LST over different periods. Although several studies have explored the relationship between landscape features and urban LST, further discussion on various aspects is needed. This study aims to investigate the influence of landscape features and land cover patterns on LST in two cities (Amman and Zarqa) in Jordan, and identify which features (vegetation cover, built-up areas, and population density) most significantly affect LST values. Al-Hameedi et al. (2022) A range of natural and anthropogenic factors were selected as risk parameters. In particular, changes in LC and LST are regarded as significant factors that have contributed to large-scale environmental changes. Edan et al. (2021) The predicted land use and its effects on the seasonal variations in LST in Al Kut, Iraq were analyzed for the summer and winter seasons. This analysis utilized Landsat TM/OLI images from the years 2000, 2010, and 2020 to assess the historical LC and LST status using remote sensing techniques'. Li et al. (2017) Landsat images were used by NDBI and unsupervised classification to map bare soil areas. Nichol & To (2012) examined the LST and stress in Hong Kong. Neteler (2010) calculated the LST of the alpine environment in the Alps mountains. Lee et al. (2012) used Landsat and ASTER data to measure LST intensity in Phoenix, Arizona. Xu (2010) The proposed Normalized Difference Impervious Surface Index (NDISI) aims to estimate impervious surfaces by utilizing Landsat imagery for Fuzhou City and Aster imagery for Xiamen City in China.Voogt & Oke (2003) Thermal remote sensing is useful for evaluating land surface temperature LST, classifying LC, and supporting climate models in urban areas. Gallo & Tarpley (1996) The correlation between Land Surface Temperature (LST) and the Normalized Difference Vegetation Index (NDVI) indicates that vegetation can mitigate LST or exert a cooling effect on the surrounding temperature.

3. Materials and Methods

3.1 Study Site

The Hashimiya District is a part of the Babylon Governorate, comprised of four administrative districts: Al-Madhatiyah, Al-Qasim, Al-Shomli, and Al-Tali'ah. Covering an extensive area of 5,170 square kilometers, Hashimiyah is strategically situated between the coordinates of 32° 5′ 50" N to 32° 30′ 22" N and 45° 12′ 2" E to 44° 24′ 22" E, located just 26 kilometers south of the historic city of Hillah, the administrative center of the governorate. Nestled along the western bank of the Hillah River an important tributary of the Euphrates Hashimiyah is bordered to the north by Al-Mahawil District and shares its northwestern boundary with Al-Hilla District. To the southwest lies the Al-Najaf Governorate, while the Al-Diwaniyah Governorate borders it to the south and southeast. This strategic location underscores Hashimiyah's significance as a vital link among the surrounding regions seen in Figure 1 (Central Bureau of Statistics Iraq, 2018).

Figure 1. Hashimiya's District Location of Iraq.

3.2 Data

The spectral reflectance arc illustrates the connection between the electromagnetic spectrum and the percentage of reflectance for a particular material. LC and LST were assessed across the study area for 10 years, from 2015 to 2025. This analysis utilized data sets from Landsat-8 LC and LST, which were acquired from the United States Geological Survey (USGS) Satellite datasets were taken on (10/3/2025 at 07:38:37 and 13/3/2015 at 07:39:18) (EarthExplorer, 2025). Datasets that used were projected to the Universal Transverse Mercator (UTM), with map projection system zone 38N, and datum of World Geodetic System 84 (WGS84). The study utilized thermal observations from Landsat 8. Thermal Infrared Sensors (TIRs) from Landsat 8 (band 10) were initially captured at 100 m spatial resolution and later resampled to 30 m, refer to Table 1 for specific details. To maintain consistency, only cloud-free data sets obtained during the Springs season (March) for each year were considered due to the strong seasonality of the study area.

Number of Bands	Wavelength (micrometers)	Resolution (Meters)
Band 1: Coastal aerosol	0.43 - 0.45	30m
Band 2: Blue	0.45 - 0.51	30m
Band 3: Green	0.53 - 0.59	30m
Band 4: Red	0.64 - 0.67	30m
Band 5: Near Infrared	0.85 - 0.88	30m
Band 6: Shortwave Infrared 1	1.57 - 1.65	30m
Band 7: Shortwave Infrared 2	Shortwave Infrared (SWIR) 2	30m
Band 8: Panchromatic	0.50 – 0.68	15m
Band 9: Cirrus	1.36 - 1.38	30m
Band 10: Thermal Infrared 1	10.6 - 11.19	100m (resampled to 30)
Band 11: Thermal Infrared 2	11.50 - 12.51	100m (resampled to 30)

Table. 1 Landsat 8 Bands Operational Land Imager and Thermal Infrared Sensor.

3 .3 Method

This research study investigated the relationship between LST and LC in Hashimiya to determine the impact of urbanization on environmental changes. LC was classified into three categories: water, vegetation, and impervious surfaces (built-up areas and bare soil) using index methods. Then, we estimated UHL for the city for two periods of time (2015-2025) to examine LCC and its relationship.

3.3.1 Indices

A. Normalized Difference Vegetation Index (NDVI) is a commonly used vegetation index for monitoring greenery globally. Healthy vegetation absorbs electromagnetic spectrum in the visible range effectively. Chlorophyll present in plants absorbs the Blue (0.4 - 0.5 µm) and Red (0.6 - 0.7 µm) spectrum and reflects the Green (0.5 – 0.6 µm) spectrum. Healthy plants also show high reflectance in the Near Infrared (NIR) range between 0.7 to 1.3 µm, due to the internal structure of plant leaves. The high reflectance in NIR and high absorption in the red spectrum are utilized to calculate NDVI. The NDVI formula uses these reflectance values to compute the index.

NDVI=(Red - NIR) / (Red+ NIR) ……………………….…Eq (1)
NDVI= (Band4- Band5) / (Band4+Band5)

Where the red band is (0.64 – 0.67 µm) reflectance and the near-infrared band is (0.85–0.88 µm) reflectance (Table 1). (Crippen, 1990)

B. Normalized Difference Water Index (NDWI) is utilized for the identification and extraction of water bodies. Its effectiveness lies in the fact that water exhibits different light reflection properties compared to land within the visible portion of the electromagnetic spectrum. Specifically, liquid water typically reflects more light in the blue spectrum (0.4 - 0.5 µm) than in the green (0.5 - 0.6 µm) and red (0.6 – 0.7 µm) spectra. Clearwater demonstrates the highest reflectance in the blue region. Furthermore, water does not reflect light in the near-infrared (NIR) spectrum or beyond. NDWI is calculated using near-infrared (NIR) and short-wave infrared (SWIR) bands, and can be determined using the following formula:
NDWI=(SWIR - Green) / (SWIR + Green) ……………………..Eq (2)
NDWI = (Band 6 – Band 3) / (Band 6 + Band 3)
Where the Short-Wave infrared (SWIR) is (1.566 – 1.651µm) reflectance and green band is (0.53 - 0.59 µm) reflectance (Table 1). (Alyasiri Elaf Amer, 2021; Gao, 1996).

C. Normalized Difference Impervious Surface Index (NDISI) refers to human-made features that impede water infiltration into the ground, such as building roofs, asphalt or cement roads, parking lots, sidewalks, and transportation infrastructure and bare soil. Impervious surfaces serve as an indicator of urbanization and are crucial for monitoring environmental issues in developed areas, including the urban heat island effect. Detecting impervious surfaces in urban regions is essential for understanding their impact. Differentiating between impervious surfaces and other land cover types, such as instructed material, sand, and bare soil in arid regions, presents challenges due to similar spectral signature values. Built-up areas, bare soil, and sand exhibit spectral response features akin to impervious surfaces, contributing to noise in previous studies. Impervious materials possess high emittance in the thermal infrared (TIR) band, low reflectance in the near-infrared (NIR) band, and stronger reflectance in the middle infrared (MIR) band.
NDISI = (Red -SWIR) / (Red - SWIR) ……………………..…… Eq (3)
NDWI = (Band 4 – Band 7) / (Band 4 + Band 7)
Where Short-Wave infrared (SWIR) is (1.566 – 1.651µm) reflectance and near-infrared NIR band is (0.85–0.88 µm) reflectance (Table 1).

3.3.2. Land Surface Temperature

LST changes with wavelength and shows the temperature of the layer in contact with the ground. When measured from the ground, air, or bare soil, LST indicates the overall surface temperature based on radiance. (Norman & Becker, 1995a). Using data acquired from the thermal infrared sensor (TIRS), Band 11 has significant uncertainty. It is recommended to use TIRS Band 10 data as a single spectral band for LST estimation (Rongali et al., 2018). The following steps were followed to generate LST from thermal bands:

Step 1: conversion of the digital number (DN) of the thermal band to Top of the Atmosphere (TOA) radiance ($L\lambda$). For Landsat 8, band 10 is considered to extract Spectral Radiance (SR) Satellite sensors measure reflectance from the earth's surface as digital numbers (DN) representing every pixel of the image (Yeneneh et al., 2022).

$L\lambda = ML * Q_{CAL} + AL - O_i$ ....Eq (4)

Where is
$L\lambda$ = Spectral Radiance of Top the atmosphere (TOA)
ML= the band specific multiplicative rescal factor Radiance multiplicative (Watts/m2*sr* µm) which is (0.0003342) (Table 2)
QCAL = Digital number (DN) of band 10
AL = the band-specific additive rescaling factor (0.1) (Table 2)
O_i = Correction value for band 10 is 0.29. (Table 2)

Rescaling Factor	Degree	Data Source
M_L (Radiance multi band)	0.0003342	Metadata
A_L (Radiance add band)	0.1	Metadata
K1 (Thermal constant)	774.8853	Metadata
K2 (Thermal constant)	1321.078	Metadata
Oi (Correction value)	0.29	Metadata

Table. 2 Rascal Factors for Landsat 8 (band 10).

Step 2: After the Digital Numbers (DN) would be converted to reflection, the TIRS band would be converted as well from spectral radiance to brightness temperature (BT) by using the thermal constants provided in the metadata file, which is calculated by using the following equation (Avdan & Jovanovska, 2016):

Kelvin (K) to Fahrenheit (ºF) Degrees BT = K2/ In (K1/Lλ+1) − 255.372 …….……..…Eq (5)
For obtaining the results in Celsius, the radiant temperature is revised by adding the absolute zero (approx. −255.372°F)
Where
BT = is Top of atmosphere brightness temperature (C)
$L\lambda$ = is TOA spectral radiance (W/ (m^2*sr*μm).
K1 = is constant Band (1321.08) (Table 2)
K2 = is constant Band (777.89) (Table 2)
λ = spectral radiance in watts per meter squared steradian micron (W/ (m^2*sr*μm).

Step 3: NDVI: which is calculated by using the following equation:
NDVI = (NIR−RED)/(NIR + RED)……..……………………….. Eq (6)
NDVI= (Band5- Band4)/(Band5+band4)

Where
RED = is DN values of the Red band.
NIR = is DN values of the Near-Infrared band.

Step 4: Proportion of Vegetation (PV) is the vegetation cover and spatial variation of the temperature of the land surface. PV is calculated by following the equation (Sobrino et al., 2004)
$PV = ((NDVI - NDVI_{min})/(NDVI_{max} - NDVI_{min}))^2$ ……………….Eq (7)

Were
PV = Proportion of Vegetation
NDIV= is DN values of NDVI
$NDVI_{min}$= is minimum DN values of NDVI images
$NDVI_{max}$= is maximum DN values of NDVI images.

Step 5: Land Surface Emissivity (E) must be known to estimate (LST), it is acquired by taking the ratio of two different emitted radiances which are the actual emitted radiance and radiance from absolutely emitting surface under the same temperature order (Norman & Becker, 1995b) agricultural areas. (*Climate Adaption Key to Iraq's Stability and Economic Development | United States Institute of Peace*, n.d.).

Desertification and lack of water are caused by river flow fluctuations rendering Iraq vulnerable to the adverse effects of climate change(Sheik Mujabar, 2019;.Avdan & Jovanovska, 2016).

Land Surface Emissivity (E) = 0.004*PV + 0.986

Were
E= is land surface emissive
PV= is Proportion of Vegetation
0.986 = is corresponds to a correction value of the equation.

Step 6: Estimating LST using the following equation proposed by (Artis & Carnahan, 1982; Yeneneh et al., 2022, (Alyasiri Elaf Amer, 2024)

LST= BT/(1+ (Lλ *BT/ C2) * In(E)) ………………………..…..…. Eq (8)
were,
LST = is land Surface Temperature;
BT = is Top of the atmosphere at brightness temperature (ºC)
Lλ = is wavelength of emitted radiance in meters
E = is land Surface Emissivity.
C2 = is h $*$ c/s = 1.4388 $*$ 10^{-2} Mk) = 14388 km
h = is Planck's Constant = 6.626*10^{-34} JS
S = is Boltzmann constant = 1.38*10^{-23} JK
C = is Velocity of Light, and 2.998 *10^{8} m/s

4. Results

In the presented research, the spatial relationship between LCC and LST will be examined to map the impact of climate change in Hashimiya district. Different index methods were used as environmental change indicators. Figure 2 is an index of water bodies in Hashimiya district for the years 2015 and 2025, which maps the main river (Hillah River) and some other water bodies. Table 3 shows the area of the classified LCC for the two selected years (2015, 2025). NDWI LC in 2015 covered about 1.1% of the area and had increased to 1.1% in 2025.

Year	**2015**		**2025**	
Area	**Km2**	**Percentage**	**Km2**	**Percentage**
NDWI	23	1.1	17.3	1
NDVI	897	53.5	894.4	53.3
NDISI	758	45.4	763.3	45.5
Sum	1675	100	1675	100

Table 3 Indices Area of Hashimiya for the Years 2015 and 2025.

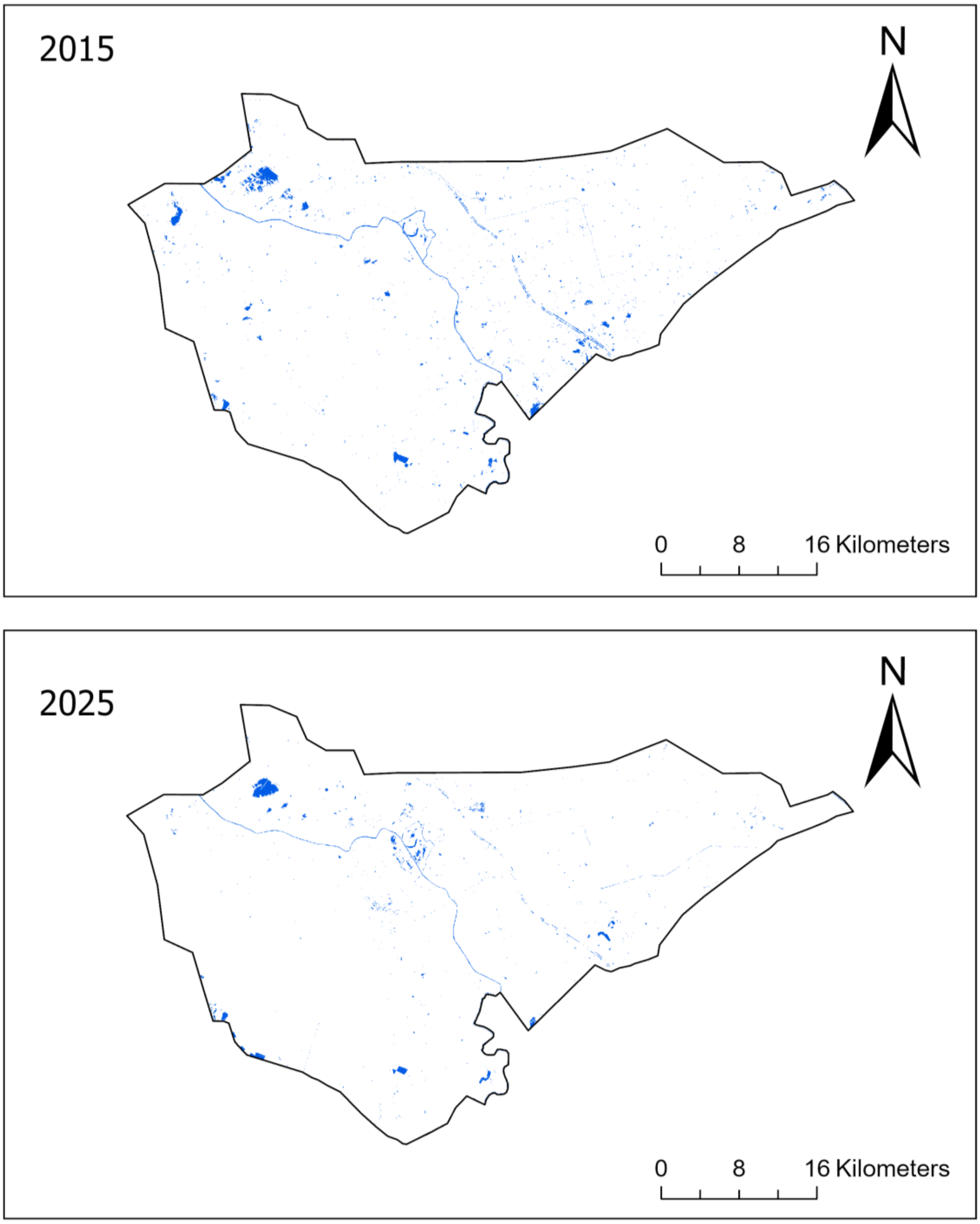

Figure .2 Normalized Difference Water Index of Hashimiya district for the years 2013 and 2023.

Figure 3 presents the vegetation index for the region around Hashimiya district for the years 2015 and 2025. As shown in Table 3, the NDVI covered approximately 53.5% of the study area in 2015. However, by 2025, this coverage had decreased to 53.3.6%. The miner decline in vegetation indicates the impact of climate change and urban sprawl.

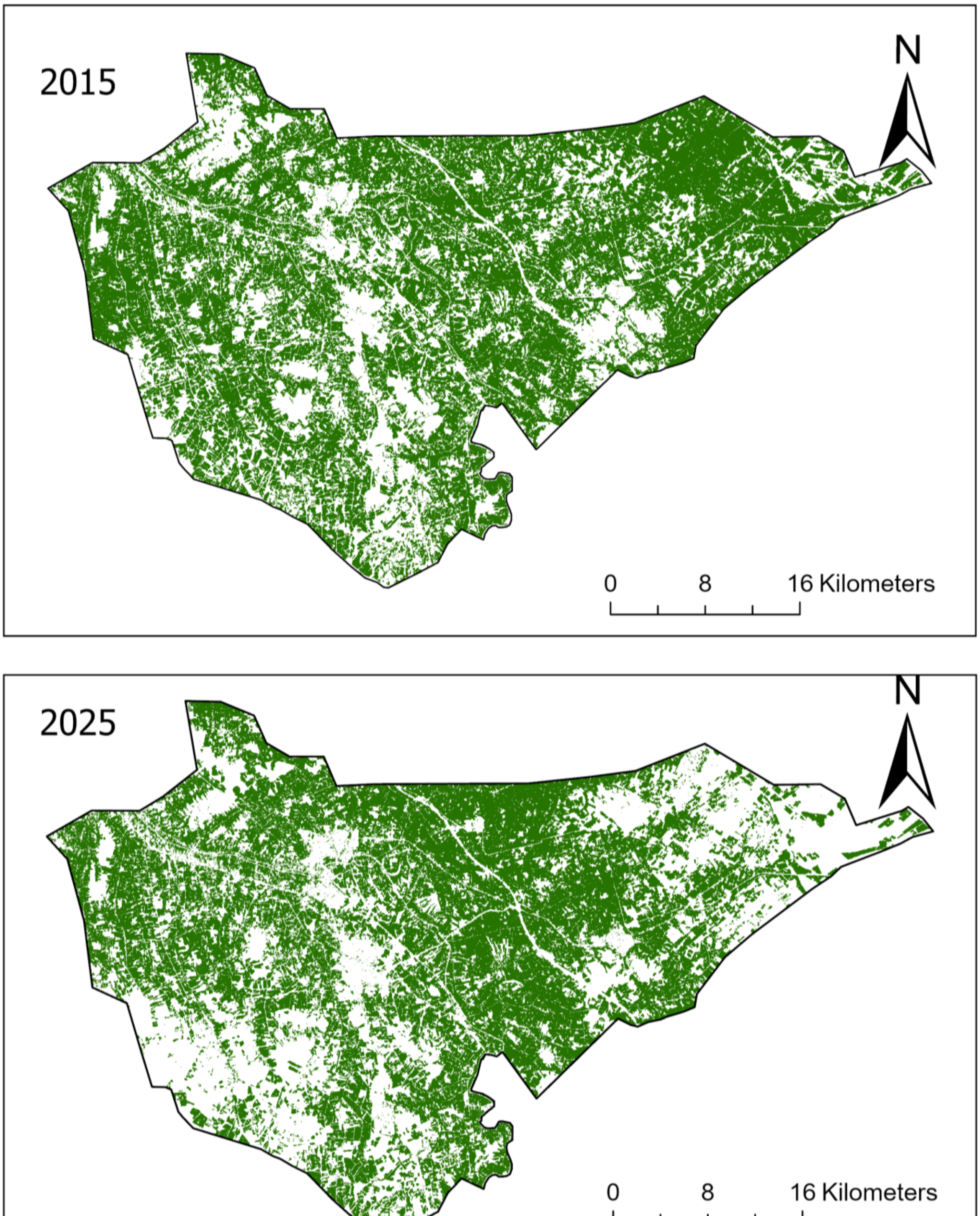

Figure .3 Normalized Difference Vegetation Index of Hashimiya Gouvernen for the years 2015 and 2025.

The NDSI of the study area for the years 2015 and 2025 is shown in Table 4. It indicates that the percentage of IS increased from 45.5.6% in 2015 to 45.4% in 2025. This rise in IS cover over vegetation suggests urbanization growth and a reduction in green areas.

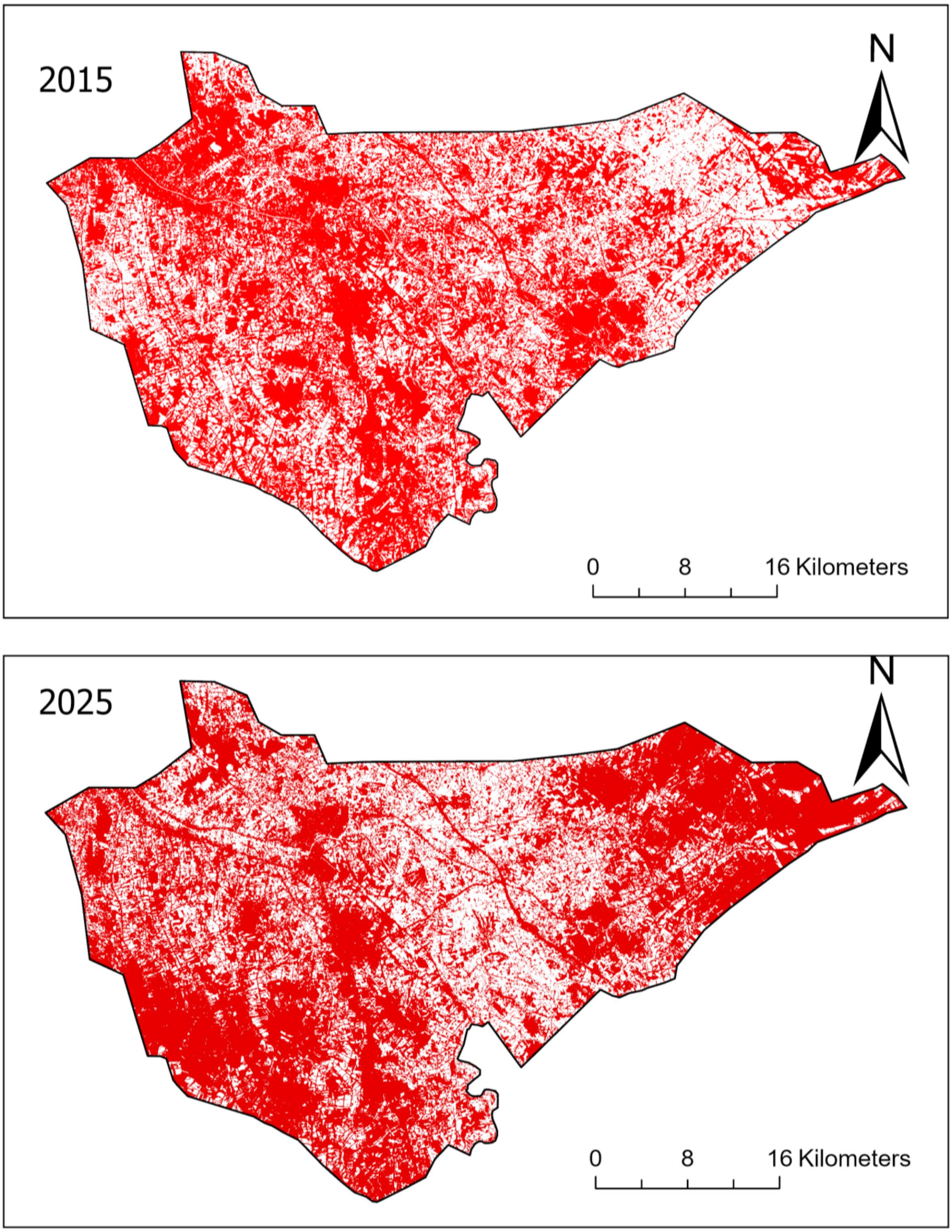

Figure .4 Normalized Difference Impervious Surface Index of Hashimiya Gouvernen for the years 2015 and 2025.

Figure 5 shows the LST in the Hashimiya district, using LST data from 2015 and 2025. According to Figure 4, temperatures in 2015 ranged from 55°F (12.7°C) to 65°F (18.3°C). In

2025, they ranged from 65°F (18.3°C) to 75°F (23.8°C). This indicates an increase in LST of about 5 degrees.
A comparison of LST with NASA Power data showed that the skin surface temperature was 21.31°C in March 2015 and dropped to 19.97°C by March 2025. This suggests a decrease in LST (Nasa Power Ceres, 2024).

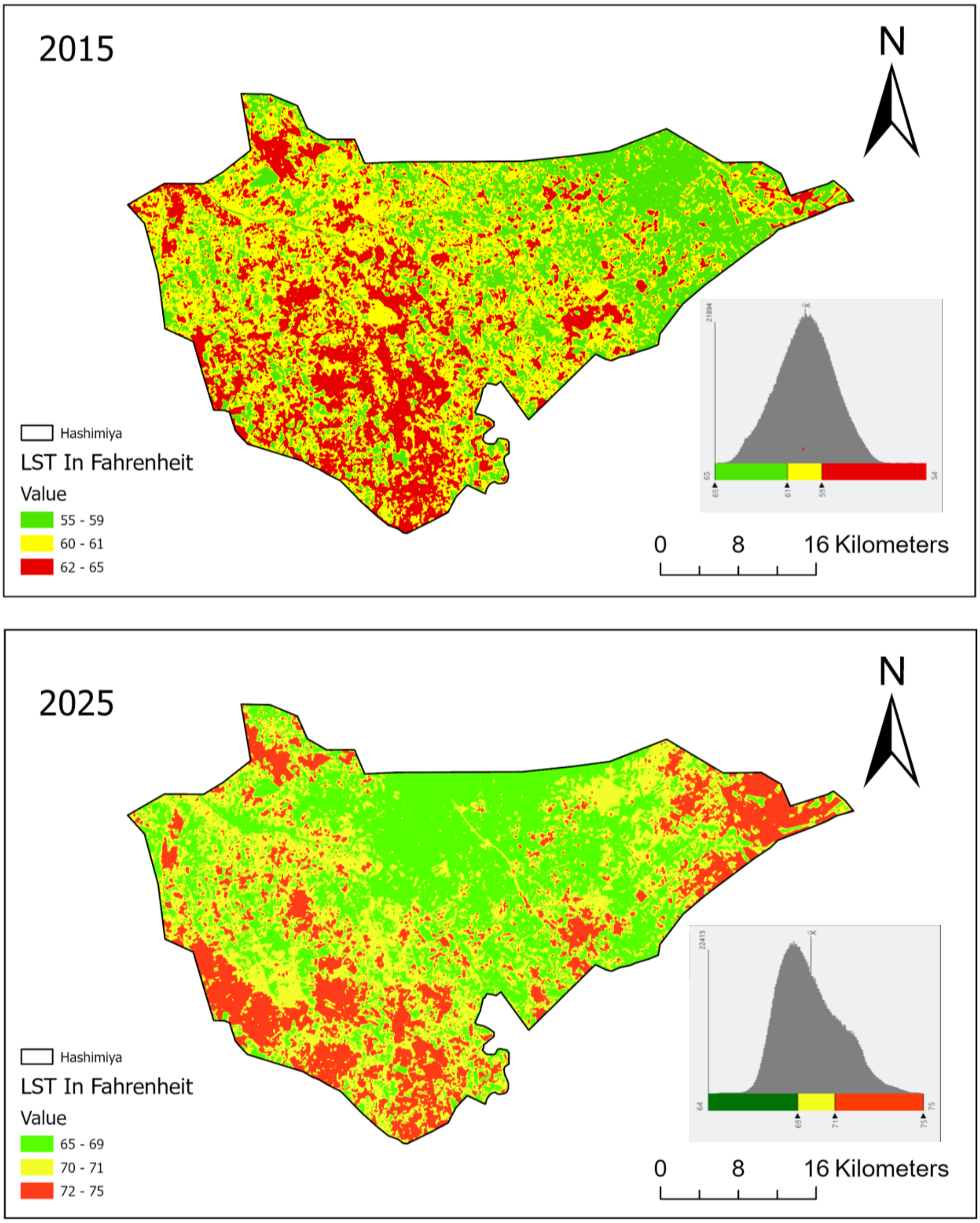

Figure .5 Land Surfers Temperature of Hashimiya District Ernest in Fahrenheit for the years 2015 and 2025

5. Discussion

The global phenomenon of climate change has been accelerating, with LCC increasing significantly over the past forty years. Figure 6 highlights slight shifts in LC in Hashimiya District, where urban areas and bare soil have replaced vegetation, contributing to the urban heat island effect and overall CC. The United States Institute of Peace predicts that Iraq will be among the top five countries most affected by climate change. Figure 5 and Table 3 show an increase in LC from 1.1% to 1% between 2015 and 2025, reflected in the water index, but the reasons for this increase are unclear.

Iraq is one of the countries that already facing water shortages and growing desertification, leading to the annual loss of up to 60,000 acres of farmland, according to reports from the Iraqi government and United Nations. Urbanization is expanding, with developed areas encroaching on vegetated regions, as shown in Table 3, supporting the report's findings. Climate change impacts are worsening yearly, and Iraq's population is expected to reach 80 million by 2050. Simultaneously, the country's resources are dwindling and encountering significant challenges. Temperatures in Iraq is rising about seven times faster than the global average, causing reduced water levels due to evaporation. Water levels in Iraq are projected to decrease by 30 to 70 percent by the end of the century. This situation calls for long-term resource management planning, especially in agricultural areas. Figure 5 shows that the land surface temperature (LST) of urban areas has increased compared to other LCs. Consequently, temperatures in 2015 ranged from 55°F (12.7°C) to 65°F (18.3°C), while in 2025, they are projected to range from 65°F (18.3°C) to 75°F (23.8°C). This indicates an approximate 5-degree increase in LST. The expansion of urban areas will worsen climate change effects and raise concerns about urban heat. Therefore, planners and the government need to promptly recognize and address these impacts.

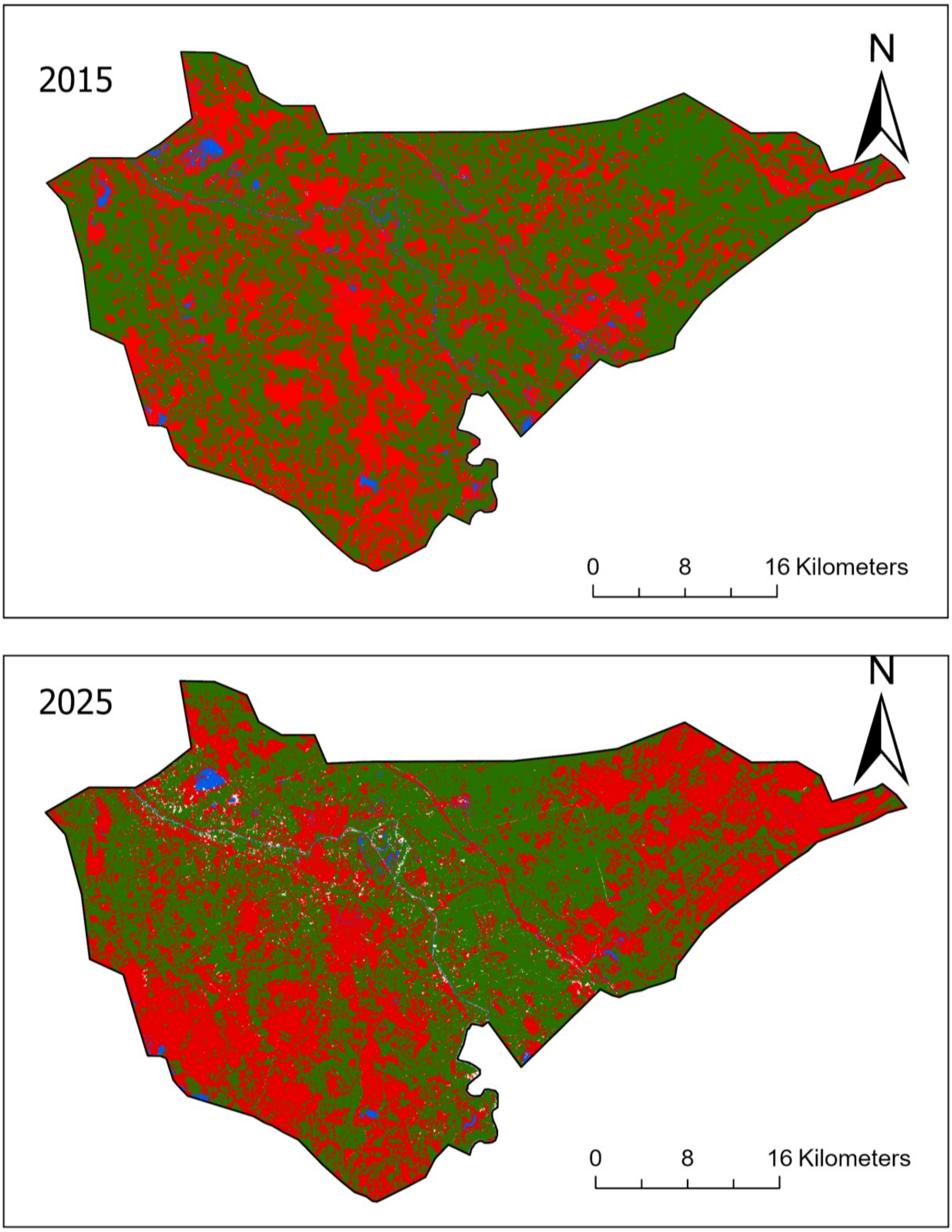

Figure. 6 Land Cover Indices of Hashimiya District the Years 2015 and 2025.

6. Conclusion

In conclusion, this study employed remote sensing applications to examine the effects of climate change on land cover (LC) and land surface temperature (LST) in the Hashimiya district. Utilizing Landsat 8 data from the years 2015 and 2025, the research aimed to assess the impact of climate change on the specified region. Various indices such as water index, vegetation index, and impervious surfaces were utilized to map LC, while LST was used to indicate urban heat temperature in Hashimiya. The findings were then compared with NASA Power data for validation; however, the results did not align. The study indicated a slight decrease in the Water Index (WI), declining from 1.1% in 2015 to 1% in 2025. Conversely, the Vegetation Index (VI) experienced a minor decrease, dropping from approximately 53.5% in 2015 to 53.3% in 2025. The Impervious Surface Index (IS) showed an upward trend, with the coverage of impervious surfaces increasing from 45.4% in 2015 to 45.5% in 2025. Furthermore, the study measured urban heat temperatures, which ranged from 55°F (12.7°C) to 65°F (18.3°C) in 2015, and increased to a range between 65°F (18.3°C) and 75°F (23.8°C) in 2025. This demonstrates an increase in LST of approximately 5 degrees. A comparison of LST with NASA Power data revealed that skin surface temperature was 21.31°C in March 2015, decreasing to 19.97°C by March 2025. This suggests a decrease in LST.

Reference

Al Shawabkeh, R., AlHaddad, M., Al-Fugara, A., Al-Hawwari, L., Al-Hawwari, M. I., Omoush, A., & Arar, M. (2024). Modeling the impact of urban land cover features and changes on the land surface temperature (LST): The case of Jordan. *Ain Shams Engineering Journal*, *15*(2), 102359. https://doi.org/10.1016/J.ASEJ.2023.102359

Al-Hameedi, W. M. M., Chen, J., Faichia, C., Nath, B., Al-Shaibah, B., & Al-Aizari, A. (2022). Geospatial Analysis of Land Use/Cover Change and Land Surface Temperature for Landscape Risk Pattern Change Evaluation of Baghdad City, Iraq, Using CA–Markov and ANN Models. *Sustainability 2022, Vol. 14, Page 8568*, *14*(14), 8568. https://doi.org/10.3390/SU14148568

Alyasiri Elaf Amer. (2021). *Remote Sensing Applications in Population Estimation, Regression Analysis, and Urban Growth Simulation Modeling for a Middle Eastern City - ProQuest*. Northern Illinois University. https://www.proquest.com/openview/bf2618fdd21e0a764aa671b894346310/1?pq-origsite=gscholar&cbl=18750&diss=y

Alyasiri Elaf Amer. (2024). *Detecting the Impact of Climate Change on Land Cover and Land Surface Temperature in Baghdad by Using Remote Sensing. 15*(2), 2464–2477.

Artis, D. A., & Carnahan, W. H. (1982). Survey of emissivity variability in thermography of urban areas. *Remote Sensing of Environment*, *12*(4), 313–329. https://doi.org/10.1016/0034-4257(82)90043-8

Avdan, U., & Jovanovska, G. (2016). Algorithm for automated mapping of land surface temperature using LANDSAT 8 satellite data. *Journal of Sensors*, *2016*. https://doi.org/10.1155/2016/1480307

Central Bureau of Statistics Iraq. (2018). 2018. https://cosit.gov.iq/ar/?option=com_content&view=article&layout=edit&id=1205

Climate Adaption Key to Iraq's Stability and Economic Development | United States Institute of Peace. (n.d.). Retrieved May 25, 2024, from https://www.usip.org/publications/2023/11/climate-adaption-key-iraqs-stability-and-economic-development#

Climate change impacts on land temperature increase. (n.d.). Retrieved May 23, 2025, from https://www.climatesignals.org/climate-signals/land-surface-temperature-increase

EarthExplorer. (n.d.). Retrieved May 21, 2024, from https://earthexplorer.usgs.gov/

Edan, M. H., Maarouf, R. M., & Hasson, J. (2021). Predicting the impacts of land use/land cover change on land surface temperature using remote sensing approach in Al Kut, Iraq. *Physics and Chemistry of the Earth, Parts A/B/C*, *123*, 103012. https://doi.org/10.1016/J.PCE.2021.103012

Gallo, K. P., & Tarpley, J. D. (1996). The comparison of vegetation index and surface temperature composites for urban heat-island analysis. *International Journal of Remote Sensing*, *17*(15), 3071–3076. https://doi.org/10.1080/01431169608949128

Gao, B. C. (1996). NDWI—A normalized difference water index for remote sensing of vegetation liquid water from space. *Remote Sensing of Environment*, *58*(3), 257–266. https://doi.org/10.1016/S0034-4257(96)00067-3

Hart, M. A., & Sailor, D. J. (2009). Quantifying the influence of land-use and surface characteristics on spatial variability in the urban heat island. *Theoretical and Applied Climatology*, *95*(3–4), 397–406. https://doi.org/10.1007/S00704-008-0017-5/METRICS

Joshi, R., Singh, A., Parab, T. P., Mandy, J. J., & Pande, C. B. (2024). *Assessing the Impact of Recent Climate Dynamics on Land Since the Last Two Decades (1991–2021) Using LST and NDVI*. 269–308. https://doi.org/10.1007/978-981-97-2879-4_14

Khandelwal, S., Goyal, R., Kaul, N., & Mathew, A. (2018). Assessment of land surface temperature variation due to change in elevation of area surrounding Jaipur, India. *The Egyptian Journal of Remote Sensing and Space Science*, *21*(1), 87–94. https://doi.org/10.1016/J.EJRS.2017.01.005

Land Surface Temperature. (n.d.). Retrieved May 23, 2025, from https://climate.esa.int/en/projects/land-surface-temperature/

Lee, S. H., Yang, J., Goddard, M. E., Visscher, P. M., & Wray, N. R. (2012). Estimation of pleiotropy between complex diseases using single-nucleotide polymorphism-derived genomic relationships and restricted maximum likelihood. *Bioinformatics*, *28*(19), 2540–2542. https://doi.org/10.1093/BIOINFORMATICS/BTS474

Li, H., Wang, C., Zhong, C., Su, A., Xiong, C., Wang, J., & Liu, J. (2017). Mapping Urban Bare Land Automatically from Landsat Imagery with a Simple Index. *Remote Sensing 2017, Vol. 9, Page 249*, *9*(3), 249. https://doi.org/10.3390/RS9030249

Li, K., Feng, M., Biswas, A., Su, H., Niu, Y., & Cao, J. (2020). Driving Factors and Future Prediction of Land Use and Cover Change Based on Satellite Remote Sensing Data by the LCM Model: A Case Study from Gansu Province, China. *Sensors 2020, Vol. 20, Page 2757*, *20*(10), 2757. https://doi.org/10.3390/S20102757

Mallick, J., Kant, Y., & Bharath, B. D. (2008). Estimation of land surface temperature over Delhi using Landsat-7 ETM+. *J. Ind. Geophys. Union*, *12*(3), 131–140.

Mansourmoghaddam, M., Rousta, I., Ghafarian Malamiri, H., Sadeghnejad, M., Krzyszczak, J., & Ferreira, C. S. S. (2024). Modeling and Estimating the Land Surface Temperature (LST) Using Remote Sensing and Machine Learning (Case Study: Yazd, Iran). *Remote Sensing 2024, Vol. 16, Page 454*, *16*(3), 454. https://doi.org/10.3390/RS16030454

NASAPOWER CERES. (2024). *POWER | Data Access Viewer*. https://power.larc.nasa.gov/data-access-viewer/

Nations, U. (n.d.). *Population | United Nations*. Retrieved May 31, 2024, from https://www.un.org/en/global-issues/population

Neteler, M. (2010). Estimating Daily Land Surface Temperatures in Mountainous Environments by Reconstructed MODIS LST Data. *Remote Sensing 2010, Vol. 2, Pages 333-351*, *2*(1), 333–351. https://doi.org/10.3390/RS1020333

Nichol, J. E., & To, P. H. (2012). Temporal characteristics of thermal satellite images for urban heat stress and heat island mapping. *ISPRS Journal of Photogrammetry and Remote Sensing*, *74*, 153–162. https://doi.org/10.1016/J.ISPRSJPRS.2012.09.007

Norman, J. M., & Becker, F. (1995a). Terminology in thermal infrared remote sensing of natural surfaces. *Agricultural and Forest Meteorology*, *77*(3–4), 153–166. https://doi.org/10.1016/0168-1923(95)02259-Z

Norman, J. M., & Becker, F. (1995b). Terminology in thermal infrared remote sensing of natural surfaces. *Agricultural and Forest Meteorology*, *77*(3–4), 153–166. https://doi.org/10.1016/0168-1923(95)02259-Z

Nouban, F., & Abazid, M. (2017). Plastic degrading fungi Trichoderma viride and Aspergillus nomius isolated fromNouban, F. and Abazid, M. (2017) 'Plastic degrading fungi Trichoderma viride and Aspergillus nomius isolated from local landfill soil in Medan', Iopscience.Iop.Org, 8(February . *Iopscience.Iop.Org*, *8*(February 2018), 68–74. https://doi.org/10.1088/1755-1315/71/1/012007/PDF

Oke, T. R., & Cleugh, H. A. (1987). Urban heat storage derived as energy balance residuals. *Boundary-Layer Meteorology*, *39*(3), 233–245. https://doi.org/10.1007/BF00116120/METRICS

Pal, S., & Ziaul, S. (2017). Detection of land use and land cover change and land surface temperature in English Bazar urban centre. *The Egyptian Journal of Remote Sensing and Space Science*, *20*(1), 125–145. https://doi.org/10.1016/J.EJRS.2016.11.003

Patel, S., Indraganti, M., & Jawarneh, R. N. (2024). A comprehensive systematic review: Impact of Land Use/ Land Cover (LULC) on Land Surface Temperatures (LST) and outdoor thermal comfort. *Building and Environment*, *249*, 111130. https://doi.org/10.1016/J.BUILDENV.2023.111130

Pengaruh, I., Dan, V., Bangunan, K., Klaten, K., Adib, M., 1✉, A., Haqqin Abrari, F., & Wibowo, A. F. (2024). Identifikasi Pengaruh Vegetasi dan Kepadatan Bangunan Kabupaten Klaten Terhadap Perubahan Suhu Melalui Citra Landsat-8 LST, NDVI, dan NDBI. *Innovative: Journal Of Social Science Research*, *4*(1), 5710–5725. https://doi.org/10.31004/INNOVATIVE.V4I1.8516

Qin, Z., & Karnieli, A. (1999). Progress in the remote sensing of land surface temperature and ground emissivity using NOAA-AVHRR data. *International Journal of Remote Sensing*, *20*(12), 2367–2393. https://doi.org/10.1080/014311699212074

Rasul, A., Balzter, H., Ibrahim, G. R. F., Hameed, H. M., Wheeler, J., Adamu, B., Ibrahim, S., & Najmaddin, P. M. (2018). Applying Built-Up and Bare-Soil Indices from Landsat 8 to Cities in Dry Climates. *Land 2018, Vol. 7, Page 81*, *7*(3), 81. https://doi.org/10.3390/LAND7030081

Rongali, G., Keshari, A. K., Gosain, A. K., & Khosa, R. (2018). Split-Window Algorithm for Retrieval of Land Surface Temperature Using Landsat 8 Thermal Infrared Data. *Journal of Geovisualization and Spatial Analysis*, *2*(2), 1–19. https://doi.org/10.1007/S41651-018-0021-Y/METRICS

Sheik Mujabar, P. (2019). Spatial-temporal variation of land surface temperature of Jubail Industrial City, Saudi Arabia due to seasonal effect by using Thermal Infrared Remote Sensor (TIRS) satellite data. *Journal of African Earth Sciences*, *155*, 54–63. https://doi.org/10.1016/J.JAFREARSCI.2019.03.008

Sobrino, J. A., Jiménez-Muñoz, J. C., & Paolini, L. (2004). Land surface temperature retrieval from LANDSAT TM 5. *Remote Sensing of Environment*, *90*(4), 434–440. https://doi.org/10.1016/J.RSE.2004.02.003

Sun, Z., Wang, C., Guo, H., & Shang, R. (2017). A Modified Normalized Difference Impervious Surface Index (MNDISI) for Automatic Urban Mapping from Landsat Imagery. *Remote Sensing 2017, Vol. 9, Page 942*, *9*(9), 942. https://doi.org/10.3390/RS9090942

Tanoori, G., Soltani, A., & Modiri, A. (2024). Machine Learning for Urban Heat Island (UHI) Analysis: Predicting Land Surface Temperature (LST) in Urban Environments. *Urban Climate*, *55*, 101962. https://doi.org/10.1016/J.UCLIM.2024.101962

Ullah, S., Ahmad, K., Sajjad, R. U., Abbasi, A. M., Nazeer, A., & Tahir, A. A. (2019). Analysis and simulation of land cover changes and their impacts on land surface temperature in a lower Himalayan region. *Journal of Environmental Management*, *245*, 348–357. https://doi.org/10.1016/j.jenvman.2019.05.063

Voogt, J. A., & Oke, T. R. (2003). Thermal remote sensing of urban climates. *Remote Sensing of Environment*, *86*(3), 370–384. https://doi.org/10.1016/S0034-4257(03)00079-8

What Is Climate Change? - NASA Science. (2025). https://science.nasa.gov/climate-change/what-is-climate-change/

Xu, H. (2010). Analysis of Impervious Surface and its Impact on Urban Heat Environment using the Normalized Difference Impervious Surface Index (NDISI). *Photogrammetric Engineering and Remote Sensing*, *76*(5), 557–565. https://doi.org/10.14358/PERS.76.5.557

Yeneneh, N., Elias, E., & Feyisa, G. L. (2022). Detection of land use/land cover and land surface temperature change in the Suha Watershed, North-Western highlands of Ethiopia. *Environmental Challenges*, *7*, 100523. https://doi.org/10.1016/J.ENVC.2022.100523